

EFFECT OF EXTERNAL MAGNETIC FIELDS ON THE OPERATION OF RF CAVITIES*

D. Stratakis[#], J. S. Berg, J. C. Gallardo, and R. B. Palmer
 Brookhaven National Laboratory, Upton, NY 11973

Abstract

Recent experiments have shown severe surface damage and a reduction of the maximum accelerating gradient for an rf cavity that is operating under external magnetic fields. This implies that serious problems may occur in lattices where rf cavities and external magnetic fields coexist, such as those of the proposed neutrino factory and muon collider. Although existing data suggest that this magnetic field dependent breakdown is associated with the emission of electrons from locally enhanced field regions on the cavity surface, the mechanism that drives this effect is not yet well understood. Here, we show that such field emitted electrons are accelerated by the cavity and focused by the magnetic field to the other side of the cavity where they heat its surface. We show that if the magnetic field is strong, significant surface deformation can occur that eventually could limit the accelerating gradient of the cavity. Results of our model are compared to the existing experimental data from an 805 MHz cavity.

INTRODUCTION

A significant effort is currently underway to explore the feasibility of designing and constructing a high luminosity muon-collider [1]. The muon beam emittance is reduced in these designs using the technique of ionization cooling. According to that method the beam passes through an absorber in which the muons lose transverse and longitudinal momentum by ionization loss. The longitudinal momentum is then restored by accelerating the beam through an rf cavity, leaving a net loss of the transverse momentum. The net ionization cooling is more efficient when the beam is strongly focused through the absorber. Because of the extension of the field lines beyond the solenoid, significant magnetic fields are present in the RF cavities. Thus, a good understanding of the operation of the RF cavities under external magnetic fields is of fundamental importance.

This work is motivated in part by the recent experimental observation in Ref. 2 of the reduction of the maximum accelerating gradient of the “pillbox” cavity by 60% in the presence of uniform, axial external magnetic fields. This gradient reduction has been associated to the emission of dark current electrons from microscopic asperities on one side of the cavity [3]. Those emitted electrons are getting focused by the magnetic field and impact the opposing cavity side where they induce surface heating that eventually leads to breakdown [3]. The question then is, how those emitted electrons can raise the

temperature, if this is sufficient to create surface damage and how this rise scales with the external magnetic field.

In this paper, we report results of simulations which not only model the “pillbox” experiment in Ref. 2, but also provide crucial information on 805 MHz cavity operation under different magnetic fields configurations and emission current intensities that can be important to design and predict results for the future lattices of the muon collider and neutrino factory. We estimate the resulting temperature rise as the field-emitted beam impacts the wall and show that it scales as the square of the external magnetic field.

EMISSION MODEL

A multicell cavity was tested in magnetic fields at the MuCool Test Area (MTA). The cavity consisted of six open 805 MHz RF cavities with vacuum windows at the ends. After some time dark current was observed and measurements revealed that it scaled as a power law, with the cavity electric field and this was reminiscent of Fowler-Nordheim (FN) emission which is described by:

$$J = 6.0 \times 10^{-12} \frac{\beta_e^{2.5} E_s^{2.5}}{\phi^{1.75}} 10^{4.52\phi^{-0.5}} \left(e^{-\frac{6.53 \times 10^9 \phi^{1.5}}{\beta_e E_s}} \right) \quad (1)$$

where J is the average current density in an RF cycle, E_s is the electric field on the cavity surface, ϕ is the metal work function and β_e is enhancement factor which is defined as the maximum local electric field divided by the average surrounding surface field. It was found [4] that the location of the window damage corresponded to magnetically focused dark current coming from one of the high field irises. From the density of the dark currents beamlets produced on the cavity window it was determined that a total of approximately 1000 emitters were present, each with a surface area of 10^{-14} m^2 . The measured emission current was 0.1-1 mA suggesting that the local field enhancement was ≈ 184 and the local field of each emitter was 4-10 GV/m [4].

In our simulation we model each individual emitter as a prolate spheroid, an approximation that is not far from the actual asperity shape. Then, in terms of the prolate spheroidal coordinates, which are defined by $z = c_2 u v$, $\rho = c_2 [(u^2 - 1)(1 - v^2)]$, the expression for the potential is

$$V(\rho, z) = E_s z \left(1 - \frac{\coth^{-1} u - \frac{1}{u}}{\coth^{-1} u_0 - \frac{1}{u_0}} \right) \quad (2)$$

*Work supported by the US Department of Energy
[#]diktys@bnl.gov

were $u_0 = \alpha / (\alpha^2 - b^2)^{1/2}$, $c_2 = \sqrt{a^2 - b^2}$, E_s is the surface field, α is the major axis and b the minor axis of the prolate spheroid. Then, in the vicinity of the asperity region the electric field along the normal and transverse directions can be described by the derivatives of this potential. To allow a more detailed comparison between experiment and theory, in our simulation we assume that the emission from asperities is governed by the FN model by using the parameters from the multi-cell experiment. The detailed emitter geometry as well as the distributions of the transverse and radial fields along the asperity and the emitted current are illustrated in Fig. 1. Note that the current is plotted within the asperity's radius of curvature.

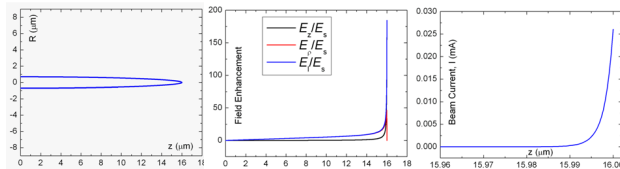


Figure 1: Geometry of the asperity assumed in the simulation (left). Field enhancement (middle) and current profile along the longitudinal asperity-axis (right).

ELECTRON MOTION AND SPACE-CHARGE EFFECTS

In Ref. 2 by tracking single electrons it was found that emitted electrons from one side of the cavity were accelerated by the rf fields, and under the influence of external fields were focused into small spots on the other side of the cavity (impact energies ≈ 1 MeV). However the previous study left several questions answered. First, those simulations were limited to single particles tracking. How will a beam distribution involve and how space-charge will influence its transport? Second, the previous simulations assumed that the beam departs from the iris. What can we learn if we track electrons from locally enhanced regions (asperities) that would resemble more conditions of relevant experiments? Third, what is the predicted temperature rise from dark currents and how it scales with the external B fields?

In an attempt address these questions we will track electrons from the asperities such as described previously. We note that the assumed cavity geometry is that of the “pillbox” 805 MHz cavity in Ref. 2. To perform the simulations we use PARMELA [5]. The code tracked the particles along a grid that is a superposition of the asperity fields and RF fields (generated by SUPERFISH). For simplicity, the asperity was placed along the cavity axis [see Fig. 2(a)].

The cavity used in our simulation as well the particle distributions at different positions are illustrated in Fig. 2. Note that the beam distribution is initially localized in a very confined region [top in Fig. 2(b)] equal to the radius of curvature (i. e. 30 nm). Because the initial energy is low (1 eV), strong repelling space-charge forces are present which in combination with the asperity radial fields give transverse momenta to emitted electrons

causing the beamlet radius to increase. However, at distances far from the source, space-charge becomes negligible and thereafter each particle moves only under the influence of the external applied fields, which in our case are the external magnetic field and the rf fields. If the magnetic field is strong enough, the beam finally becomes focused to a small spot on the opposing cavity wall [bottom in Fig. 2(b)].

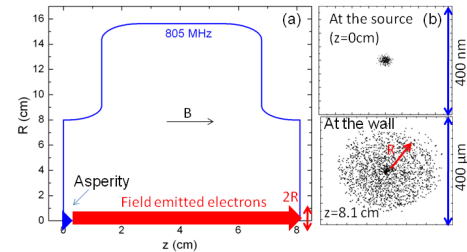


Figure 2: Simulation details: (a) The 805 MHz cavity; (b) Beam distributions at different positions. Distances are not drawn to scale.

Now we will examine the dependence of the final beamlet radius to the B field and the beam current. When the beam is relativistic, space-charge becomes negligible however, near the emission point where the electron beam energy is low space-charge becomes comparable to the external fields. Assuming that the beam is matched with zero emittance and zero canonical angular momentum the

beam radius is given by $R \propto \frac{\sqrt{I}}{B}$. A simple simulation

was performed [6] to test the accuracy of this expression. First a flat emission point (no asperity) was assumed. A fit to the data revealed that $R \propto \sqrt{I}/B$ as predicted. Then, in order to resemble more closely the experimental conditions, the flat emitter was replaced by the asperity in Fig. 1 and the simulation was repeated. The presence of strong radial electric fields in the asperity case provided an outward “kick” to the electrons that in turn reduced the space-charge effects. A fit to the data revealed that now

the beam radius scales as $R \propto \frac{I^{0.33}}{B}$. Note that this

result was independent of the asperity dimensions and the external magnetic fields.

As the beam approaches the far side of the cavity, it's surface is getting bombarded by electrons. The power per unit area of the electron beam hitting the opposing surface is given by $W_s = \frac{P}{(\pi R^2)}$ were P is the incident power. As

those electrons penetrate inside the metal they gradually lose energy. In Ref. 6, the electron penetration depth in Cu for typical operation acceleration gradients of the 805 MHz pillbox cavity was examined in great detail.

SURFACE DEFORMATION

As the beam penetrates inside Cu the energy is deposited inside the metal. At the same time heat is also

flowing out of this region following the equation of the heat diffusion. The power absorbed within a thin region close to the surface, provides a reasonable estimate of the surface temperature rise [3]. This thin region can be approximated by the diffusion length, $\delta = \sqrt{D\tau}$ with D and τ being the thermal diffusion constant and RF pulse respectively. Since the RF pulse at 805 MHz is approximately 20 μs [3] the diffusion depth for Cu becomes 48 μm . We note that the penetration depth was between 100-1000 μm [6], thus it's much larger than the diffusion length. This suggests that only a fraction of incident power will be deposited at the surface. From the heat conduction equation and by assuming that the temperature remains uniform within the thermal diffusion length [6] the surface temperature rise becomes $\Delta T = W_\delta \frac{\tau}{\rho C_s}$, where $W_\delta = \frac{\chi W_s}{\delta}$ is the power

density deposited within the diffusion length, ρ is the material density, and C_s is the specific heat. Note that χ is a dimensionless parameter used to define the fraction of the incident energy deposited in δ . Then the temperature rise in terms of the magnetic field can be written as

$$\Delta T \propto \frac{\chi E_e I^{0.34}}{\pi \delta \rho C_s} \tau B^2.$$

We now turn on to estimate the temperature rise for the 805 MHz cavity, whose physics is of interest due to the observed breakdown with magnetic field in the pillbox cavity experiment as stated earlier. We record temperatures for different fields and gradients that are typical parameters of this cavity and our results are shown in Fig. 3. Interestingly, for lower gradients (i.e. $E_s=16.5$ MV/m) the predicted rise is below 100 $^\circ\text{C}$ but still breakdown occurred in the experiment. Given that the melting temperature for Cu is 1085 $^\circ\text{C}$, this result suggests that most likely the driving mechanism for breakdown is not melting.

Pulse heating experiments [7] showed significant material damage on Cu samples that were heated in the range of 40 to 110 $^\circ\text{C}$. The damage was attributed due thermal cyclic fatigue. Specifically, the metal heats up and cools down in between the pulses. Since the lateral dimensions of the surface layer are constrained by the bulk metal, the heating, instead of causing dimensional changes, induced lateral internal stress, and corresponding strain. As the number of pulses increased those strains induced fatigue and eventually micro cracks occurred [7]. In Fig. 3 we record the magnetic fields were the limiting temperatures of 40 and 110 $^\circ\text{C}$ were reached for each surface gradient in the pillbox cavity. In the same plot we record (with a black square) the measured breakdown gradient in the MTA experiment. As is apparent from Fig. 3 the breakdown points lie within or close to the ranges where fatigue is expected for Cu.

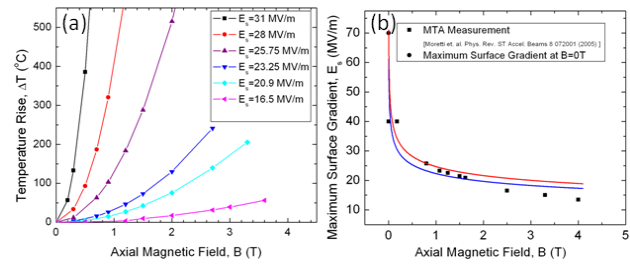


Figure 3: (a) Predicted by simulation temperature rise for the 805 MHz cavity; (b) Comparison with experiment.

SUMMARY

The geometry of the pillbox cavity in our case is more complicated, and the analysis depends on the electron energies, focused dimensions, and angle of impact, but damage may reasonably be expected with similar cyclical heating above 40 $^\circ\text{C}$. However, it is not yet known what the mechanism is for such surface damage to cause a cavity to breakdown. One possibility is that if electrons are focused on a location with a high surface gradient, then the local damage will generate new asperities with higher FN enhancement factors, thus initiating breakdown.

While our preliminary analysis offers some quantification on the effects of the magnetic fields on the cavity's operation, other theoretical issues were not addressed. For instance, emission from secondary electrons was disregarded, the asperity was placed on axis, the magnetic field was assumed as uniform, the thermal-diffusion calculation ignored the shape of the rise time, and adopted an approximate calculation. On the theoretical level, it will be interesting to pursue additional simulations exploring these effects in detail. Experimentally, there is a clear need for more well-designed experiments to study, systematically, the effect of external fields on the cavity's operation.

The authors are grateful to S. G. Tantawi, V. A. Dolgashev, L. Laurent, J. Norem, A. Bross and A. Moretti.

REFERENCES

- [1] R. B. Palmer et al. of the 2007 Particle Accelerator Conference p. 3193.
- [2] A. Moretti, et al. , Phys. Rev. ST 8, 072001 (2005).
- [3] R. B. Palmer, R. C. Fernow, J. C. Gallardo, D. Stratakis, and D. Li, Phys. Rev. ST. Accel. Beams 12, 031002 (2009).
- [4] J. Norem, et al. Phys. Rev. ST. Accel. Beams 6, 072001 (2003).
- [5] L. Young and J. Billen, Proceedings of the 2003 Particle Accelerator Conference p. 3521 (2003).
- [6] D. Stratakis, J. S. Berg J. C Gallardo, R. B. Palmer, in preparation.
- [7] D. P. Pritzkau and R. H. Siebman, , Phys. Rev. ST. Accel. Beams 5, 112002 (2002); S. G. Tantawi et al. Proceedings of PAC07, Albuquerque, NM, p. 2370.